

Investigation of Stress Intensity Factor Reduction using Steel and GFRP Patches for Repairing Edge Cracks in Steel Plates

Zainab Najih Jassam ^{1,*}, Rafil M. Laftah ²^{1,2,3} Department of Mechanical Engineering, College of Engineering, University of Basrah, Basrah, IraqE-mail addresses: zainabnajih30@gmail.com, rafil.laftah@uobasrah.edu.iq

Received: 17 July 2023; Revised: 17 August 2023; Accepted: 28 August 2023; Published: 15 February 2024

Abstract

The ultimate objective of this study was to compare the performance of repaired edge cracks in steel plates before and after repair with patches made of steel patch and glass fiber-reinforced polymer composite patches (GFRP) in different shapes: circular, rectangular, and trapezoidal, under two conditions: unsymmetric patch (one patch) and symmetric patch (two patches). A three-dimensional finite element model of the one-sided and two-sided repaired examples is used to study how the steel and composite patch affect the stress intensity factor (SIF). Under uniaxial tensile loads, the use of steel patches and GFRP composite patches to repair cracks was studied. The results showed that the steel patch performs better than the GFRP patch because it significantly lowers the stress intensity factor (SIF). The symmetric patch arrangement (two patches) is better than the un-symmetric patch arrangement (one patch) because it significantly reduces the stress intensity factor (SIF).

Keywords: Fracture mechanics, SIF, GFRP, Different shape patches.

<https://doi.org/10.33971/bjes.24.1.2>

1. Introduction

Adhesive-bonded composite patches are commonly used to repair cracked machines or structural components [1]. Advanced composite materials offer advantages for structural repairs, including high specific strength, stiffness, corrosion resistance, and fatigue characteristics. Furthermore, the patches can be made in various sizes and shapes to accommodate complex geometries and features. Additionally, by modifying the volume fraction of the reinforcement and the lay-up of plies, the rigorous criteria of strength and stiffness in various directions can be met [2]. In the last few decades, much research has been done on how to make damaged buildings last longer. For example, many studies have been done on how to make cracked metal structures last longer and handle damage better in an efficient and cost-effective way. Because composites are light, stiff, and robust without being too heavy, a repair method that uses a composite patch to strengthen a cracked structure is very hopeful [3–5]. In the early 1970s, Baker and Jones [6], who were the first to use bonded patches to repair things, researched this technology extensively. They talked about the benefits of using composite material patches to repair metal structures that have been damaged or split [7]. A recent study shows that applying adhesives is an effective way to repair cracked structures by making the damaged parts last longer before they break down. It has been demonstrated that using composite patch material to repair cracks lowers the stress at the crack tips. Cracked parts of a structure last longer when composite repairs are put on either one or both sides [8–10]. An analogous computational investigation performed by Umamaheswar and Singh [11] similarly indicated a clear correlation between adhesive thickness and the decrease in SIF. As SIF governs the extent of damage, its progression

beyond the material's fracture toughness can potentially result in structural failure [12].

The study's major goal is to investigate how a patch's presence affects the stress intensity factor. ABAQUS software uses the Extended Finite Element Method (XFEM) to calculate the SIF values and fracture toughness on punched plates with different hole shapes, sizes, and arrangements [13, 14].

2. Geometrical model

The main plate used in this investigation was a steel plate with uneven edge crack lengths. The crack was repaired using steel and glass fibre reinforced polymer (GFRP) composite patches in different shapes, circular, rectangular, and trapezoidal, under two conditions: unsymmetric patch (one patch) and symmetric patch (two patches), as shown in Fig. 1.

Table 1 contains the entirety of the data that pertains to the geometry of the main plate and the patch.

The ABAQUS application uses a three-dimensional finite element method (3D-FEM) to demonstrate the effect of steel and GFRP patches on the process of repairing a cracked steel plate.

The main plate of steel alloy is modeled as an isotropic material in a computer simulation. The adhesive layer and steel patch were modeled as an isotropic material within the property module of ABAQUS/Standard [15]. Steel and GFRP make the patch's composition, and GFRP was modeled as a composite layup within the layup module. The mechanical and material properties of the steel plate, steel patch, adhesive layer, and glass/epoxy composite patch are listed in Table 2.

The mechanical properties of Glass epoxy composite repair wrap material, and film adhesive epoxy FM 73 are derived from ref [16].

Table 1. Geometry (main steel plate, steel patch, GFRP patch)

Symbol	Value	Description
hp	200	The height of the steel plate (mm)
W	100	The width of the steel plate (mm)
t	4	The thickness of the main plate (mm)
a	(5, 10, 15, 25, 30)	Crack length (mm)
h	100	The height of the patch (mm)
w _p	50	The width of the patch (mm)
t _p	2	The thickness of the steel patch (mm)
t _{cp}	0.2	The thickness of each layer of the GFRP patch (mm)
t _{ah}	0.1	The thickness of the adhesive (mm)
Angle (θ)	[90], [0/45/-45/90]	Stacking composite laminate sequence (degree)
N _p	4	Number of GFRP patch layers

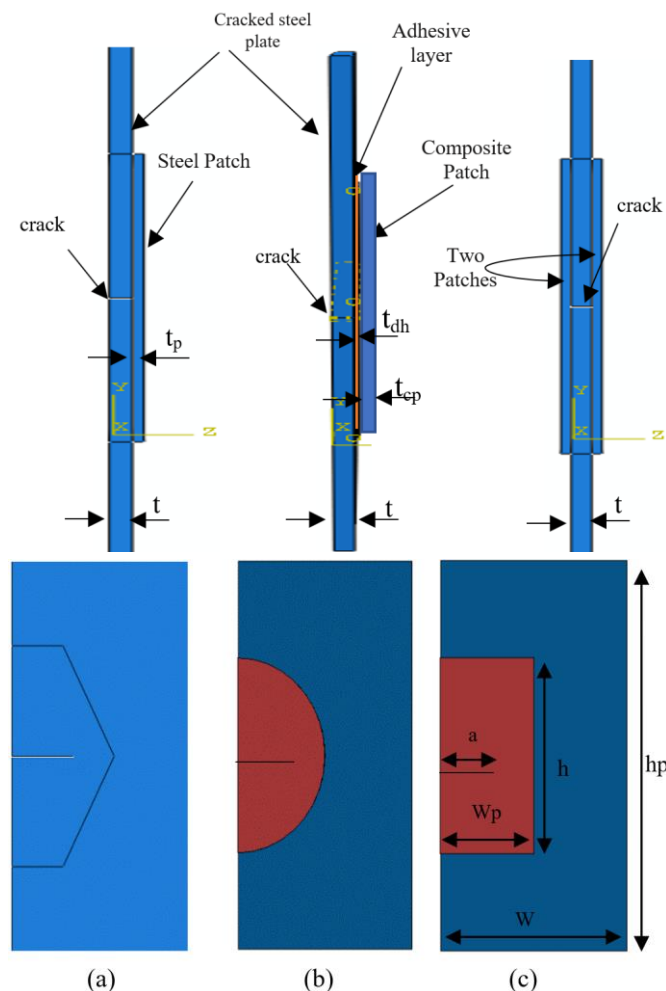


Fig. 1 Geometrical model of the plate with one and two patches: (a) main plate with trapezoidal patch, (b) main plate with circular patch, (c) main plate with rectangular patch.

A uniaxial tensile load of 1 MPa is applied to the plate in the uniaxial direction. The crack on the plate is covered by the steel patch and composite patch that has been bonded to the surface. All of the layers that make up the composite patch are thought to have established a full link with one another. In

addition, the tie contact option that is available in ABAQUS/Standard was utilized in conjunction with film adhesive epoxy in order to attach the composite patch to the steel plate [17].

Table 2. Material properties of the steel plate, steel patch, adhesive layer, and glass/epoxy composite patch

Symbol	Value	Property
Glass epoxy composite repair wrap material's properties.		
E_{11}	27.82	Young's modulus in fiber direction (GPa)
E_{22}	5.83	Young's modulus in the transverse direction (GPa) (In Y direction)
E_{33}	5.83	Young's modulus in the transverse direction (GPa) (In Z direction)
G_{12}	2.56	In-plane shear modulus (GPa) (X-Y plane)
G_{13}	2.56	In-plane shear modulus (GPa) (X-Z plane)
G_{23}	2.24	In-plane shear modulus (GPa) (Y-Z plane)
ν_{12}	0.31	Poisson's Ratio (X-Y plane)
ν_{13}	0.31	Poisson's Ratio (X-Z plane)
ν_{23}	0.41	Poisson's Ratio (Y-Z plane)
Steel plate and steel patch properties		
E	210	Young's modulus (GPa)
ν	0.3	Poisson's ratio
Film adhesive FM 73 material's properties		
E	1.83	Young's modulus (GPa)
ν	0.33	Poisson's Ratio

The stress intensity factor was calculated using the Extended Finite Element (XFEM) method for the steel patch and the traditional FEM method for the composite patch, in different shapes, circular, rectangular, and trapezoidal. The C3D8 (8-node linear brick) model was used to mesh each element in the steel plate, steel patch, composite patch, and adhesive under the specified boundary conditions and loading parameters. As shown in Fig. 2.

The value of the mesh has been determined by the mesh steady method, and when the stress intensity factor (SIF) is stable at a number of elements = 170929, as shown in Fig. 3.

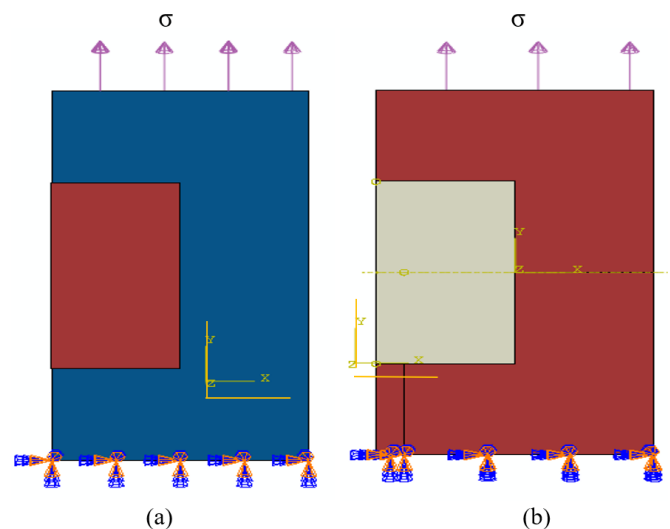


Fig. 2 Boundary conditions for finite element model. (a) steel patch, (b) composite patch.

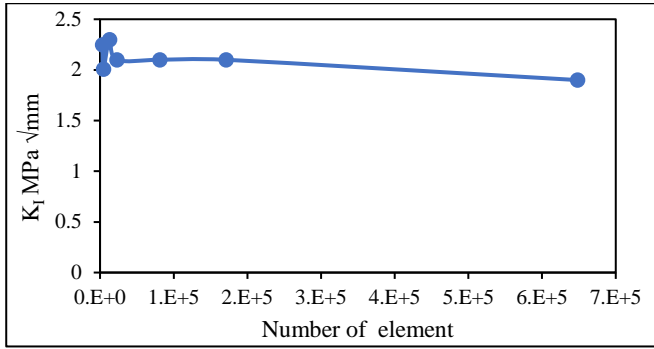


Fig. 3 Mesh steady method.

4. Results and discussion

The study aims to determine the stress intensity factor at the cracked tip before and after repair with patches made from steel patch and GFRP composite patch under two conditions: unsymmetric patch (one patch) and symmetric patch (two patches) in ABAQUS utilizing traditional FEM and XFEM.

4.1. Cracked plate before repairing (without patch)

ABAQUS's mesh structure is used to model how the stress intensity factor varies with crack length. SIF for edge-cracked steel plates can be calculated using via Eq. (1), (2) and (3) [18].

$$k_I = y \sigma \sqrt{\pi a} \tag{1}$$

$$y = 1.12 - 0.23 \left(\frac{a}{w}\right) + 10.6 \left(\frac{a}{w}\right)^2 - 21.7 \left(\frac{a}{w}\right)^3 + 30.4 \left(\frac{a}{w}\right)^4 \tag{2}$$

$$k_n = \sigma \sqrt{\pi a} \tag{3}$$

Where, y is the shape factor

Figure 4 displays the analytical and numerical values of the stress intensity factor (SIF) for an edge-cracked plate at a pressure of 1 MPa plotted against the aspect ratio (a/w) for five different crack lengths (5, 10, 15, 25, and 30 mm). The analytical and numerical values correspond quite well, as seen in Fig. 4. Figure 5 depicts the stress distribution around the crack tip.

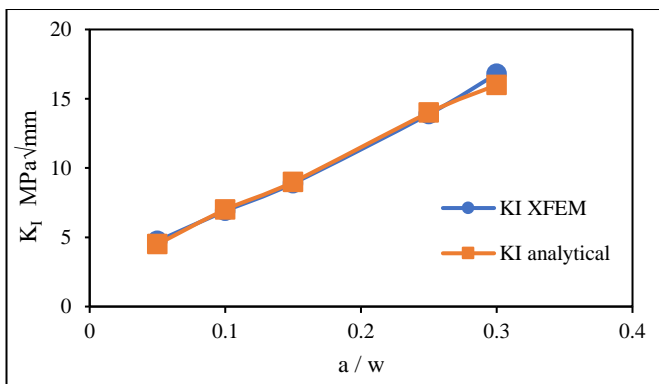


Fig. 4 Effect of crack length on the SIF of steel plate (without patch).

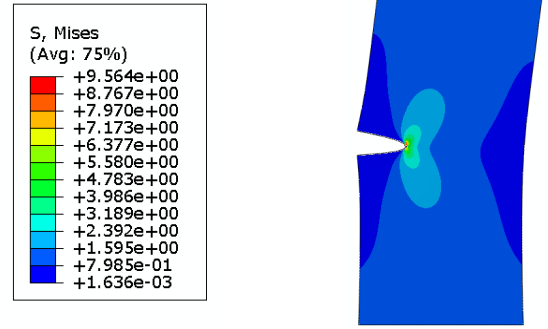


Fig. 5 Stress distribution in a cracked plate (without patch).

4.2. Cracked plate repair with steel patch

The evolution of the stress intensity factor as a function of crack length and patch shape is shown in Fig. 6. One patch, known as an asymmetric patch, was applied on one side of the plate, while two patches, known as symmetric patches, were applied on the other two sides. From Fig. 6, it can be observed that the circular and rectangular patches are stable compared to the trapezoidal patches. In the case of the one and two patches, the best results have been obtained by the circular patch.

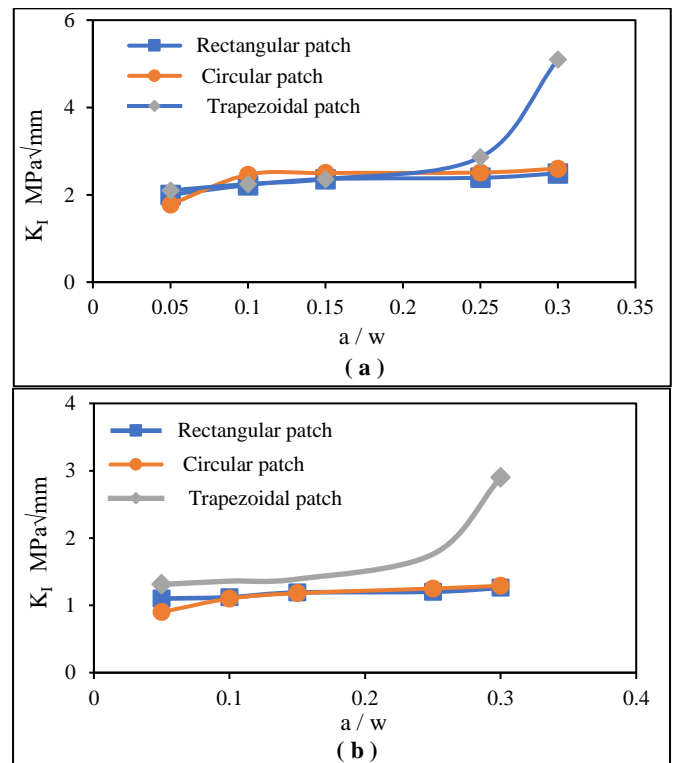
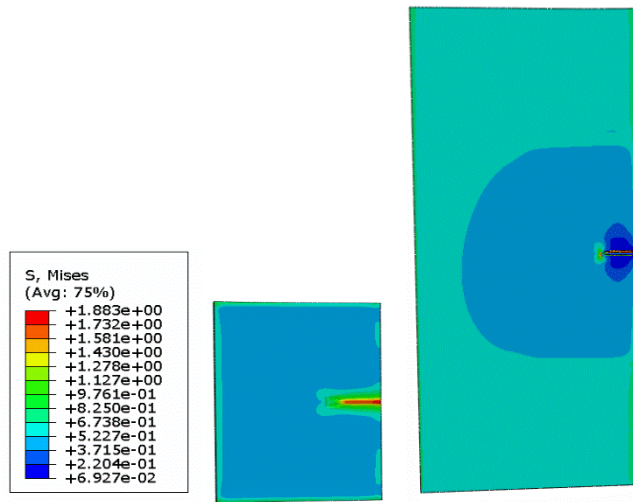
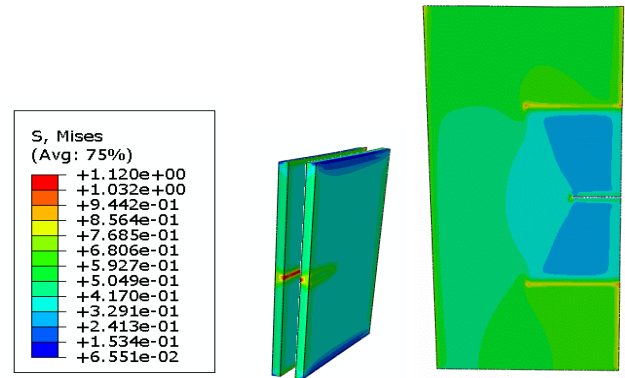


Fig. 6 Effect of crack length on the SIF with different shapes of patches: (a) unsymmetric (one patch), (b) symmetric (two patches)

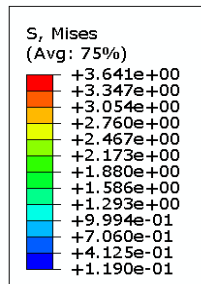
Figures 7 and 8 depict the stress distribution around the crack tip in various steel patch shapes, circular, rectangular, and trapezoidal for one and two patches.



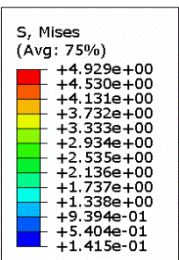
(a)



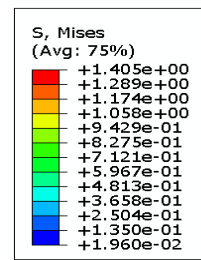
(a)



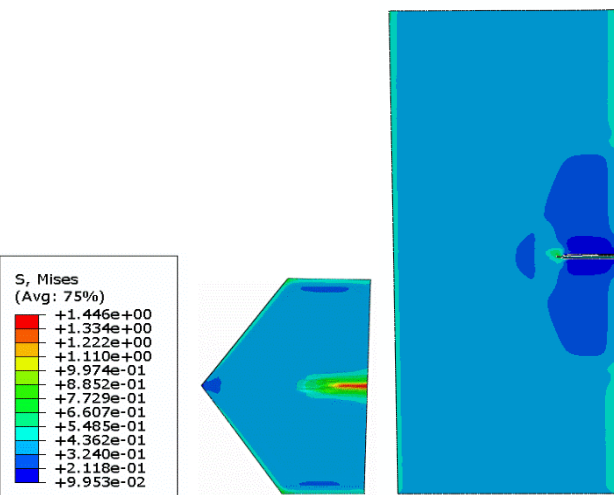
(b)



(b)



(c)



(c)

Fig. 7 Stress distribution in a cracked plate with different shapes for steel patch (one patch) (a) rectangular patch, (b) circular patch, (c) trapezoidal patch.

Fig. 8 Stress distribution in a cracked plate for steel patch (two patches): (a) rectangular patch, (b) circular patch, (c) trapezoidal patch.

From Fig. 9, it can be observed that two patches show better results compared to one patch. In other words, the two patches have significant effects on the stress intensity factor (SIF).

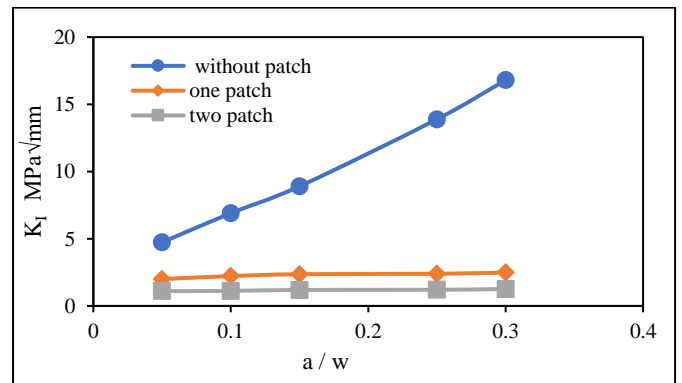


Fig. 9 Effect of unsymmetric (one patch) and symmetric (two patches) on the SIF for steel patch.

4.3. Cracked plate repair with GFRP patch

The evolution of the stress intensity factor (SIF) as a function of crack length for various GFRP patch forms (rectangular, circular, and trapezoidal) and various stacking composite laminate sequences of repair patch [90] and [0/45/-45/90] with a constant number of layers, $N = 4$, as shown in Fig. 10. The stress intensity factor increases with an increase in the ratio of crack length to crack width (a/w). As a result, increasing the value of crack length leads to an improvement in the functionality of the composite patch. The repaired patch's stacked composite laminate sequence has the highest potential to exert its beneficial effect in the uniaxial direction [90]. This potential is due to the patch's uniaxial orientation. The composite patch with the lowest efficiency is the one that uses the stacking composite laminate sequence [0/45/-45/90].

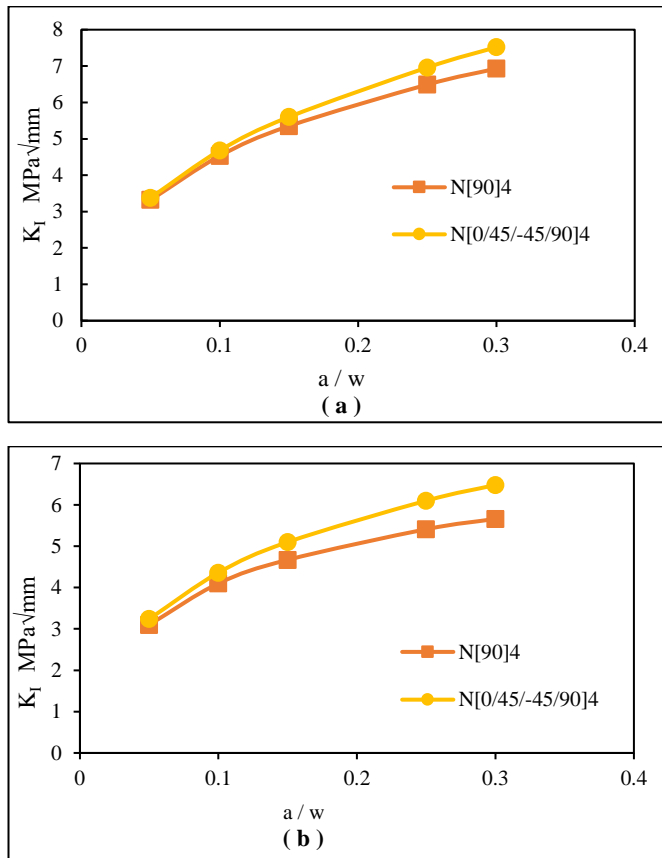


Fig. 10 Effect of Stacking composite laminate sequence on the SIF (rectangular patch): (a) unsymmetric patch (one patch), (b) symmetric patch (two patches)

From Fig. 11, it is evident that the stress intensity factor SIF values for rectangular, circular, and trapezoidal patches are stable, and there is no variation in the results. As a result, the shape of the GFRP patch does not affect the stress intensity factor (SIF).

Figure 12 shows a comparison between the efficacy of the one and the two patches on the stress intensity factor for the rectangular GFRP patch. The two patches are more efficient than the one patch.

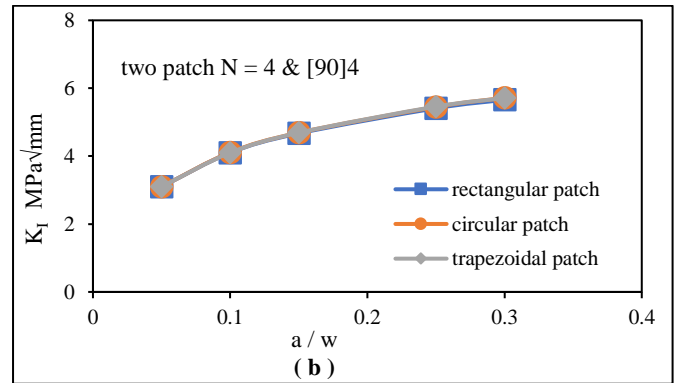
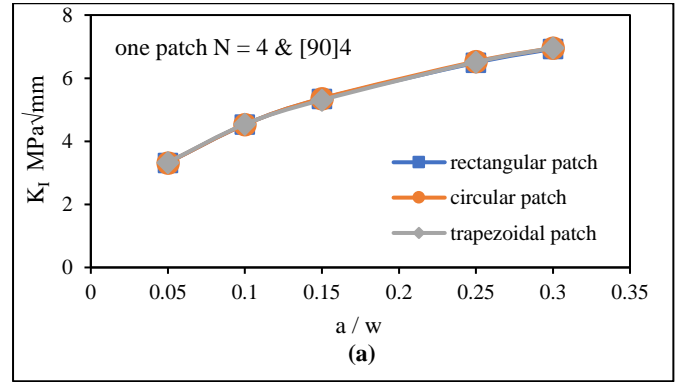


Fig. 11 Effect of crack length on the SIF (rectangular patch): (a) unsymmetric patch (one patch), (b) symmetric patch (two patches).

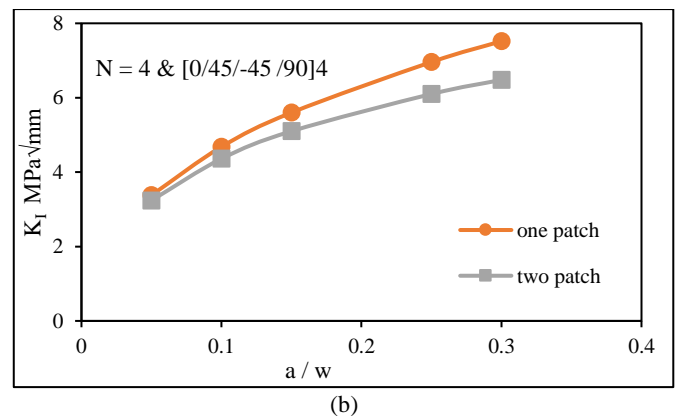
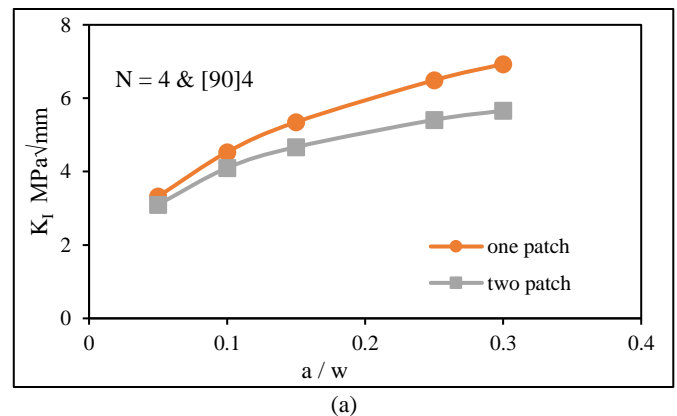
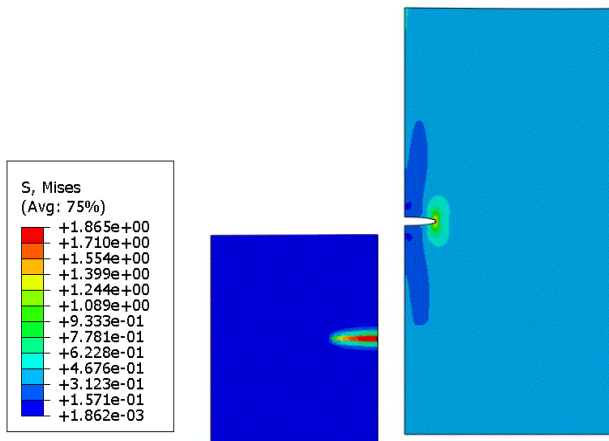
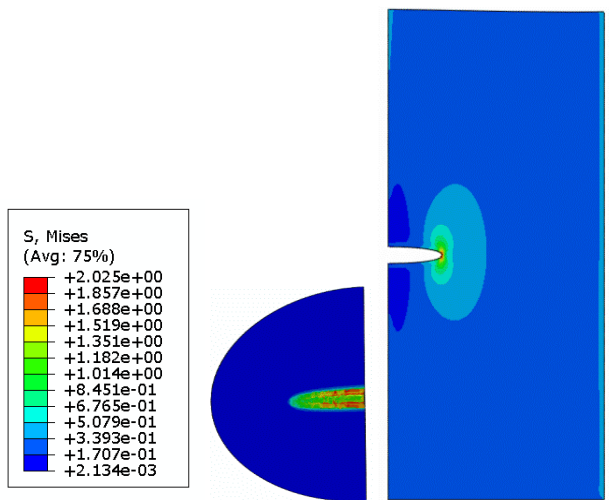


Fig. 12 Effect of unsymmetric (one patch) and symmetric (two patches) on the SIF for the rectangular GFRP patch (a) $N = 4$ & [90], (b) $N = 4$ & [0/45/-45/90].

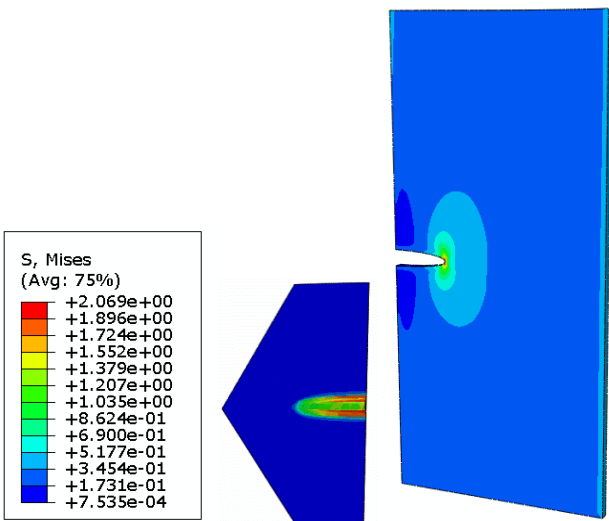
Figures 13 and 14 depict the stress distribution around the crack tip in various composite patch shapes, circular, rectangular, and trapezoidal for one and two patches.



(a)

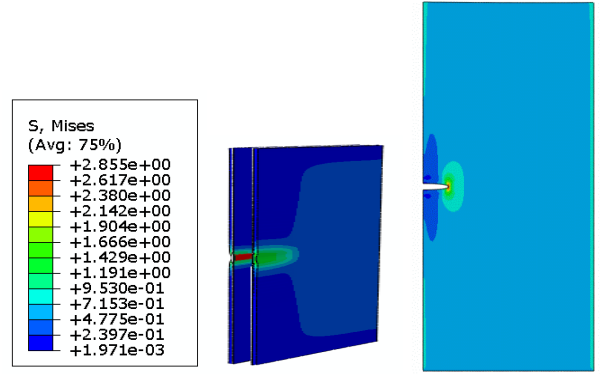


(b)

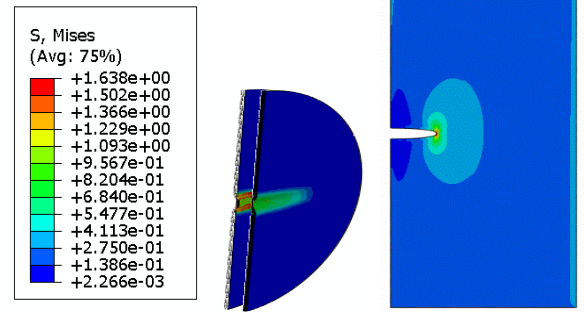


(c)

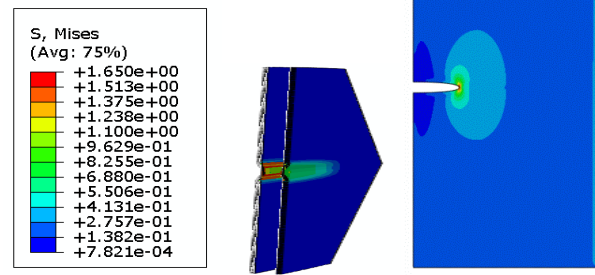
Fig. 13 Stress distribution in a cracked plate for a composite patch (one patch). (a) rectangular patch, (b) circular patch, (c) trapezoidal patch.



(a)



(b)



(c)

Fig. 14 Stress distribution in a cracked plate for a composite patch (two patches). (a) rectangular patch, (b) circular patch, (c) trapezoidal patch.

5. Comparative study

To evaluate the efficiency of steel patches and glass fiber-reinforced polymer composite patches (GFRP), we will take the rectangular, circular, and trapezoidal patches for each one and see how they perform compared to the unsymmetric patch (one patch) and symmetric patch (two patches), as shown in Figs. 15 and 16. The steel patch is more effective than the GFRP patch because it significantly reduces the stress intensity factor (SIF). The stress intensity factor (SIF) also changes considerably between the behavior with and without patches. Indeed, from Tables 3, 4, 5, and 6 it can be concluded that one patch reduced the SIF by almost (58-85%) for a rectangular steel patch, (62-85) for a circular steel patch, and (55-69%) for trapezoidal steel patch, while it decreased by (28-58%) for rectangular, circular and trapezoidal composite patches. Two patches reduced the SIF by almost (77-92%) for a rectangular steel patch, (81-92%) for a circular steel patch, and (72-82%) for a trapezoidal steel patch, while it decreased by (33-66%) for a rectangular, circular and trapezoidal composite patches. The reduction ratio for one and two patches can be calculated using via Eq. (4) and (5).

$$\text{reduction ratio \%} = \frac{K_I (\text{without patch}) - K_I (\text{one patch})}{K_I (\text{without patch})} \times 100 \quad (4)$$

$$\text{reduction ratio \%} = \frac{K_I (\text{without patch}) - K_I (\text{two patch})}{K_I (\text{without patch})} \times 100 \quad (5)$$

Table 3. The reduction ratio for the rectangular steel patch.

a / w	reduction ratio % (one patch)	reduction ratio % (two patches)
0.05	58	77
0.1	68	84
0.15	73	87
0.25	83	91
0.3	85	92

Table 4. The reduction ratio for the circular steel patch.

a / w	reduction ratio % (one patch)	reduction ratio % (two patches)
0.05	62	81
0.1	64	84
0.15	72	87
0.25	82	91
0.3	85	92

Table 5. The reduction ratio for the trapezoidal steel patch.

a / w	reduction ratio % (one patch)	reduction ratio % (two patches)
0.05	55	72
0.1	67	80
0.15	73	84
0.25	79	87
0.3	69	82

Table 6. reduction ratio for the rectangular, circular, and trapezoidal composite patches.

a / w	reduction ratio % (one patch)	reduction ratio % (two patches)
0.05	28	33
0.1	34	40
0.15	40	48
0.25	54	60
0.3	58	66

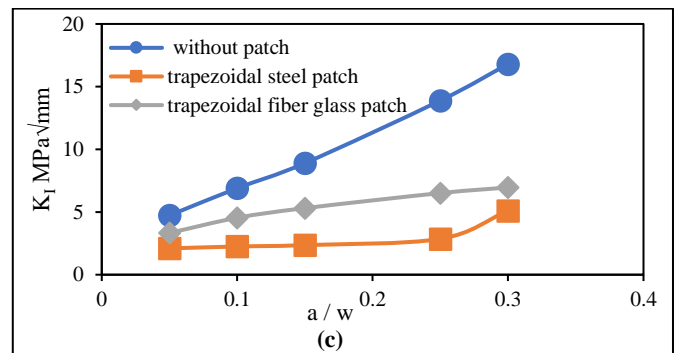
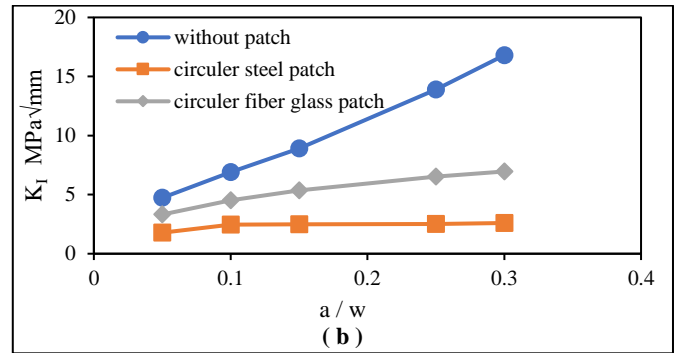
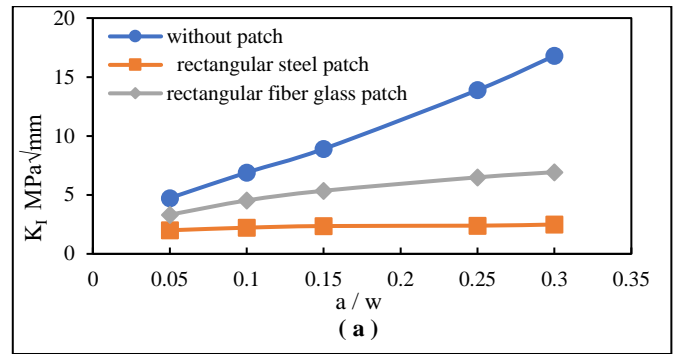
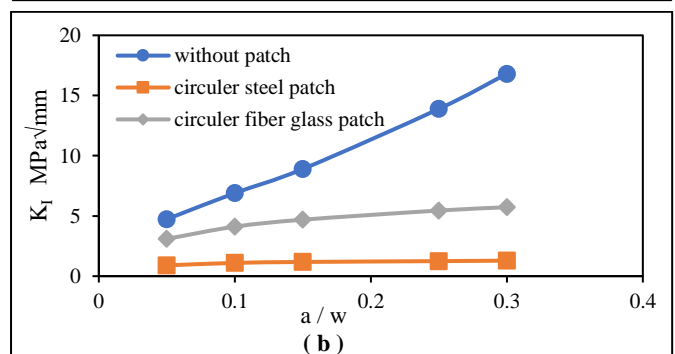
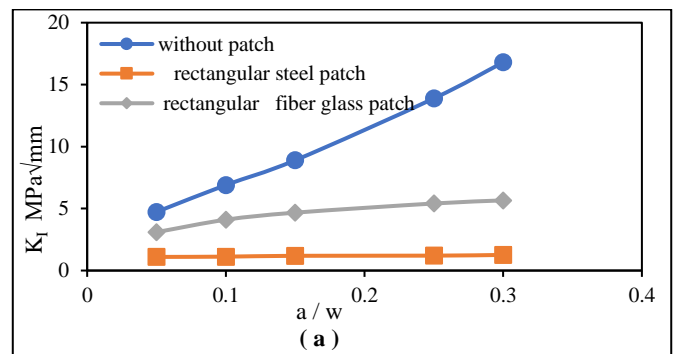


Fig. 15 Evolution of SIF as a function of the crack length for repaired and non-repaired plates, unsymmetric patch (one patch): (a) rectangular patch, (b) circular patch, (c) trapezoidal patch.



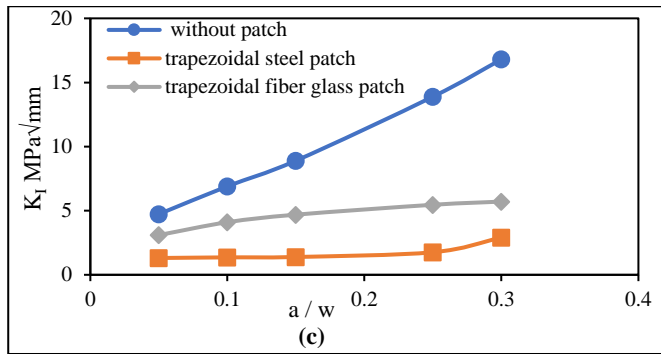


Fig. 16 Evolution of SIF as a function of the crack length for repaired and non-repaired plates, symmetric patch (two patches): (a) rectangular patch, (b) circular patch, (c) trapezoidal patch.

6. Conclusion

The following conclusion can be drawn from the most current numerical studies:

1. The efficiency of the steel patch depends on the shape and thickness of the patches. Among the various patch shapes, circular patches are more effective than rectangular and trapezoidal patches, reducing the SIF by nearly (62–85%) for one patch and (81–92%) for two patches; rectangular patches reduce the SIF by about (58–85%) for one patch and (77–92%) for two patches; trapezoidal patches reduce the SIF by nearly (55–69%) for one patch and (72–82%) for two patches.
2. The symmetric patch (two patches) configuration is the most efficient over the un-symmetric patch (one patch) because it reduces the SIF by the highest value.
3. The orientation of the fibers in the composite patch plays a significant role in the effectiveness of the patch. Layering the composite laminate sequence of the repaired patch in the uniaxial direction [90] provides the best effect, as it lowers the SIF by around (28–58%) for one patch and by (33–66%) for two patches for all of the different types of GFRP patches.
4. The shape of the GFRP patch does not affect the stress intensity factor (SIF) values.
5. Steel patches present the highest stress intensity factor (SIF) reduction, making them more effective than GFRP patches.

References

- [1] A. A. Baker, L. R. F. Rose, R. Jones, *Advances in the bonded composite repair of metallic aircraft structure*, Elsevier Applied Science Publishers, 2002. ISBN 0-08-042699-9 <https://doi.org/10.1016/B978-008042699-0/50003-6>
- [2] S. M. R. Khalili, R. Ghadjar, M. Sadeghinia, R. K. Mittal, "An experimental study on the Charpy impact response of cracked aluminum plates repaired with GFRP or CFRP composite patches", *Composite Structures*, Vol. 89, Issue 2, pp. 270-274, 2009. <https://doi.org/10.1016/j.compstruct.2008.07.032>
- [3] A. A. Baker, R. J. Callinan, M. J. Davis, R. Jones, J. G. Williams, "Repair of mirage III aircraft using the BFRP crack-patching technique", *Theoretical and Applied Fracture Mechanics*, Vol. 2, Issue 1, pp. 1-15, 1984. [https://doi.org/10.1016/0167-8442\(84\)90035-1](https://doi.org/10.1016/0167-8442(84)90035-1)
- [4] A. A. Baker, "Repair of cracked or defective metallic components with advanced fiber composites an overview of Australian work", *Composite Structures*, Vol. 2, Issue 2, pp. 153-181, 1984. [https://doi.org/10.1016/0263-8223\(84\)90025-4](https://doi.org/10.1016/0263-8223(84)90025-4)
- [5] A. A. Baker, "Bonded composite repair for fatigue-cracked primary aircraft structure", *Composite Structures*, Vol. 47, Issue 1-4, pp. 431-443, 1999. [https://doi.org/10.1016/S0263-8223\(00\)00011-8](https://doi.org/10.1016/S0263-8223(00)00011-8)
- [6] A. A. Baker, R. Jones, *Bonded repair of aircraft structures*, Springer Dordrecht, 1988. ISBN 978-94-009-2752-0, <https://doi.org/10.1007/978-94-009-2752-0>
- [7] M. R. Ayatollahi, R. Hashemi, "Computation of stress intensity factors (KI, KII) and T-stress for cracks reinforced by composite patching", *Composite Structures*, Vol. 78, Issue 4, pp. 602-609, 2007. <https://doi.org/10.1016/j.compstruct.2005.11.024>
- [8] S. N. Atluri, *Structural integrity & durability*, Tech Science Press, 1997. ISBN 0965700119
- [9] K. Kaddouri, D. Ouinas, B. B. Bouiadra, "FE analysis of the behaviour of octagonal bonded composite repair in aircraft structures", *Computational Materials Science*, Vol. 43, Issue 4, pp. 1109-1111, 2008. <https://doi.org/10.1016/j.commatsci.2008.03.003>
- [10] M. Meriem-Benziane, S. A. Abdul-Wahab, H. Zahloul, B. Babaziane, M. Hadj-Meliani, and G. Pluinage, "Finite element analysis of the integrity of an API X65 pipeline with a longitudinal crack repaired with single- and double-bonded composites", *Composites Part B: Engineering*, Vol. 77, pp. 431-439, 2015. <https://doi.org/10.1016/j.compositesb.2015.03.008>
- [11] T. V. R. S. Umamaheswar, R. Singh, "Modelling of a patch repair to a thin cracked sheet", *Engineering Fracture Mechanics*, Vol. 62, Issue 2-3, pp. 267-289, 1999. [https://doi.org/10.1016/S0013-7944\(98\)00088-5](https://doi.org/10.1016/S0013-7944(98)00088-5)
- [12] T. L. Anderson, *Fracture mechanics - fundamentals and applications*, Third Edition, CRC Press, Taylor and Francis Group, 2005. ISBN 9780429125676 <https://doi.org/10.1201/9781420058215>
- [13] M. Eftekhari, A. Baghbanan, and H. Hashemolhosseini, "Determining stress intensity factor for cracked brazilian disc using extended finite element method", *International Journal of Scientific Engineering and Technology*, Vol. 3, Issue 7, pp. 890-893, 2014.
- [14] A. O. Mashjel, R. M. Laftah, and H. I. Khalaf "Study the effect of perforation type for plate with central crack on the stress intensity factor using the XFEM", *Basrah Journal for Engineering Sciences*, Vol. 21, No. 1, pp. 27-37, 2021. <https://doi.org/10.33971/bjes.21.1.5>
- [15] D. Systèmes, *ABAQUS/Analysis User's Guide*, Version 2016, Waltham, Massachusetts, Dassault, 2016.
- [16] N. Deghoul, H. Errouane, Z. Sereir, A. Chateaneuf, S. Amziane, "Effect of temperature on the probability and cost analysis of mixed-mode fatigue crack propagation in patched aluminium plate", *International Journal of Adhesion and Adhesives*, Vol. 94, pp. 53-63, 2019. <https://doi.org/10.1016/j.ijadhadh.2019.05.004>
- [17] I. El-Sagheer, M. Taimour, M. Mobtasem, and A. Abd-Elhady, "Finite Element analysis of the behavior of bonded composite patches repair in aircraft structures", *Frattura ed Integrità Strutturale*, Vol. 14, No. 54, pp. 128-135, 2020. <https://doi.org/10.3221/IGF-ESIS.54.09>
- [18] H. I. Khalaf, "Crack Propagation in Plane Stress Problems by Using Experimental and Extended Finite Element Method (XFEM)", Ph.D. thesis, Mechanical Engineering Department, College of Engineering, University of Basrah, 2015.